Hydrology and Earth System Sciences, 8(6), *1129–1140* (2004) © EGU

Hydrology & Earth System Sciences

Simulation of flood reduction by natural river rehabilitation using a distributed hydrological model

Y.B. Liu[1], S. Gebremeskel[1], F. De Smedt[1], L. Hoffmann[2] and L. Pfister[2]

[1]Department of Hydrology and Hydraulic Engineering, Vrije Universiteit Brussel, Pleinlaan 2, 1050 Brussels, Belgium

[2]CREBS-Cellule de Recherche en Environnement et Biotechnologies, Centre de Recherche Public – Gabriel Lippmann, 162a Avenue de la Faiencerie, L-1511, Luxembourg

E-mail for corresponding authors: yongbliu@vub.ac.be, fdesmedt@vub.ac.be

Abstract

The effects of river rehabilitation on flood reduction in the Steinsel sub-basin of the Alzette River basin, Grand-Duchy of Luxembourg, are discussed; the rehabilitation measures include planting and changing riparian and in-stream vegetation, and re-meandering of channelised reaches, etc. in the headwater streams. To simulate flood reduction by river rehabilitation, the streams have been classified into different orders and by assessing the response of the stream channels to the resistance or obstruction of flows. Based on this assessment, the roughness to the flow in the first and second order streams is adjusted in line with the river rehabilitation while the roughness of higher order channels downstream is unchanged. The hydrological analysis utilises the WetSpa distributed model based on spatial information on topography, soil type and land use. The increased channel roughness in the headwater channels delays the flows, so that peak discharges at the outlet of the basin are reduced. The simulation indicates that, after river naturalisation, the reduction in peak flow can be as much as 14% and the time of concentration may be delayed by as much as two hours. Also, an impact analysis has assessed the possible flood reduction for a changed climate scenario.

Keywords: river rehabilitation, flood reduction, distributed hydrological modelling, WetSpa

Introduction

The River Alzette, one of the main tributaries of the Rhine, has experienced serious floods since the early 1990s and floods in 1993, 1995 and 1998 caused extensive damage to properties in municipal areas (Pfister *et al*., 2000). In addition to the positive trend in winter rainfall totals due to an increase in westerly atmospheric fluxes since the 1970s (Pfister *et al*., 2000), the change in land-use patterns in the Alzette basin is a major reason for rapid runoff into channelised streams, which may increase flood frequency and enhance flood peaks downstream. Moreover, urbanisation in the basin increased by 30% between 1954 and 1979 and by a further 15% between 1979 and 1995. Major changes in future land use are also expected.

Changes in land-use patterns in a catchment and especially those adjacent to rivers and streams influence hydrological processes in rivers. For instance, cropland increases runoff due to the removal of native vegetation and soil compaction; this, in turn, decreases the soil infiltration capacity. Urbanisation enhances runoff because of impervious areas, reduced vegetation cover, depression storage and the concentration and accumulation of runoff in sewage systems. Such effects increase the volume of surface runoff as well as the velocity and concentration time of storm runoff, while reducing infiltration into the soil and, ultimately, baseflow. Urbanisation can also damage the zone surrounding the channel that influences the hydrology and ecology and, therefore, reduces the amount of wood and vegetation that help to dissipate the flow energy.

For centuries, the valleys of the upper Alzette have been densely populated. Considerable modification of rivers and their riparian areas has been undertaken and physical degradation, particularly since the 1950s, has resulted from artificial drainage and flood defence structures; similar changes occurred also in the headwater areas of the basin. Because of the change in response to rainfall of a basin following urbanisation, peak flows became higher than in the pre-development stage. Previous studies have shown

the negative effect of heavily urbanised areas on peak runoff in small streams in the vicinity of the city of Luxembourg (Pfister *et al*., 2002).

Channelisation is one of the common approaches taken to reduce floods caused by urbanisation of a basin. However, flood conveyance benefits of channelisation are often offset by ecological losses resulting in an increased stream velocity and reduced habitat diversity. Channelisation, by creating faster flows, also increases the risk of flooding downstream. Because of these negative effects, there is a trend to restore streams to their pristine conditions to minimise similar flood repercussions in the future. Riparian vegetation has a strong influence on the headwater streams; it plays a key role in delaying the stream water and has major impacts on lowland stream ecosystems. Increasing the capacity of high water retention in non-critical areas may reduce the extent of flooding in the inhabited areas downstream and improve the ecological stabilisation of the watercourse. The goal of stream rehabilitation is to restore the stream to a more natural form so as to create environmentally favourable conditions; this does not necessarily imply that the stream will be restored to its pre-settlement condition (Morris, 1995). Yet the consequence will be to reduce damage to property and risk of accident, while making water flow rates more favourable to the development of aquatic life and minimising damage due to destructive erosion.

This paper investigates the effect of conceptual headwater rehabilitation measures on flooding in the Steinsel sub-basin of the Alzette basin, located mainly in Luxembourg. The naturalisation is considered for first and second-order streams, characterised by moderately steep slopes, flowing through forest and grassland intermixed with agricultural and urban areas and, therefore, potentially suitable for river rehabilitation. The simulations illustrate the importance of headwater rehabilitation on the reduction of flood peak discharge for the main channels downstream. The analysis uses the WetSpa model, a GIS-based distributed runoff and flow routing model calculating hourly runoff occurring at any point in a catchment and providing spatially distributed hydrological characteristics in the river basin. The paper neither addresses the biological and ecological value of river rehabilitation, nor does it focus on the planning and design of future river naturalisation activities.

Materials and methods

STUDY AREA AND DATA AVAILABILITY

The Steinsel sub-basin of the Alzette, situated partly in the south of the Grand Duchy of Luxembourg and partly in France, covers an area of 408 km^2 (Fig. 1). Most of the

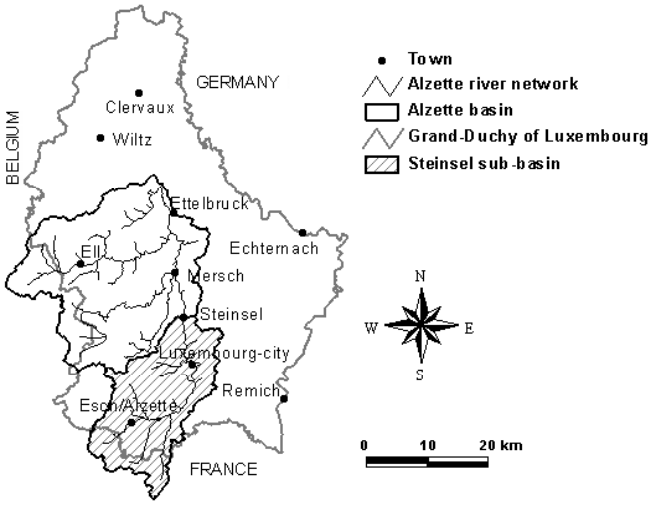

Fig.1. *Location of the Alzette basin and the Steinsel sub-basin*

Steinsel sub-basin relief is characterised by cuestas, where large flat areas of marls alternate with deep valleys cut into the Luxembourg sandstone. The study area ranges in elevation from 225 to 450 m (Fig. 2a), with an average basin slope of 0.07. The dominant soil types on the higher terrains are loamy sand (29.1%) and silt (37.7%) and, in the river valleys, silt clay loam (13.3%), sandy clay loam (10.2%) and clay loam (9.5%) The Steinsel sub-basin is one of the most urbanised areas in the Grand-Duchy of Luxembourg; it includes the city of Luxembourg in the downstream, and Esch-Alzette in the upstream, part of the sub-basin (Fig. 2b). Urban areas cover about 20.5% of the sub-basin, cultivated lands about 23.2% with main crops of maize and wheat; forest (24.3%) and grassland (29.0%) are predominant on the high terrains, intermixed with urban areas and cultivated land. Some former mining areas, about 2.5% of the total area, are located in the upstream part of the catchment which is well drained with a dense stream network. Open water surfaces such as lakes and ponds occupy about 0.5% of the total area.

The climate of the region has a northern humid oceanic regime without extremes. Rainfall is distributed relatively uniformly throughout the year. High runoff occurs in winter because soils are saturated and evapotranspiration is low while, in summer, runoff is low due to the higher evapotranspiration. According to Pfister *et al*. (2002), in recent years the maximum stormflow coefficient, which is the maximum slope of the double-mass curve of rainfall and stormflow, is stable for each sub-catchment of the Steinsel sub-basin from one winter to the next. The maximum stormflow coefficient for the upper part of the basin (sandy soils, deciduous shrub mixed with agricultural land) is 0.29, whereas the lower part has a maximum

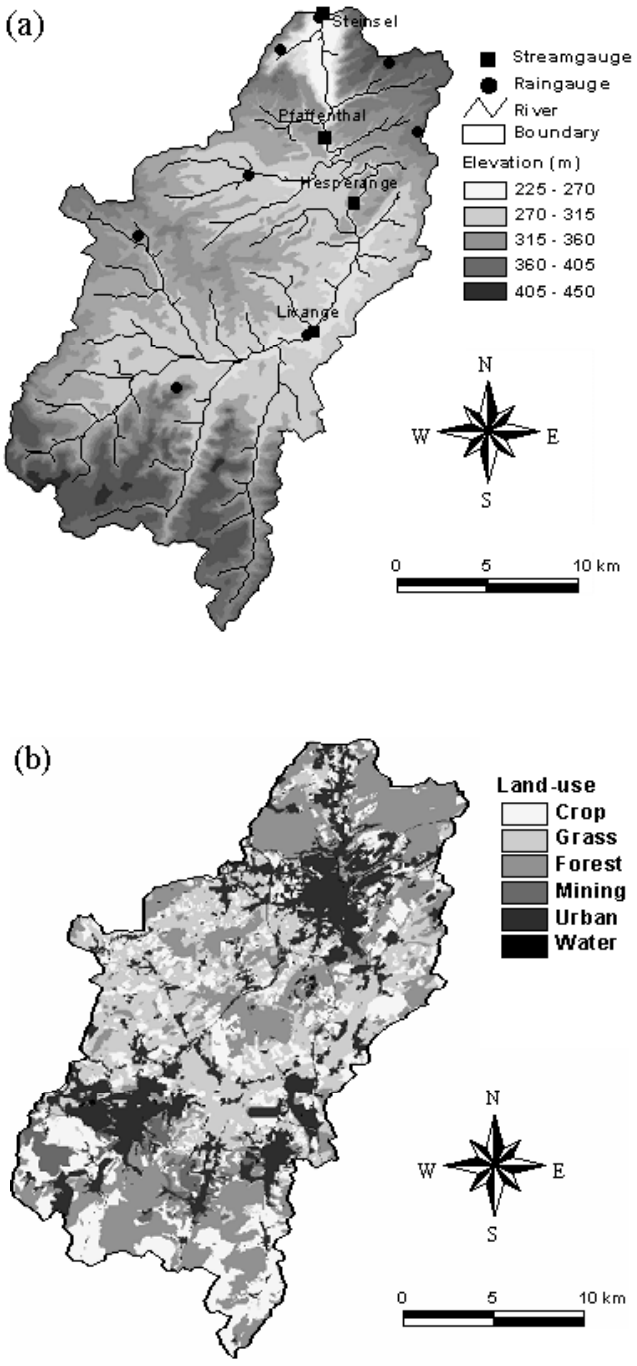

Fig. 2. *Gauging network, topography (a) and land-use (b) of the Steinsel sub-basin*

stormflow coefficient of up to 0.64, due to the extensive sewage system of Luxembourg City. The average stormflow coefficient is 0.37 for the entire Steinsel sub-basin. The maximum stormflow coefficient is related strongly to such basin characteristics as the shape of the drainage area, topography, soil type, land-use, etc.

The observation network in the Steinsel sub-basin (Fig. 2a.) comprises four stream gauges recording water level every 15 minutes on the main channel at Steinsel, Pfaffenthal, Hesperange and Livange and four hourly and six daily rain gauges are distributed in the basin. Daily rainfall records were disaggregated into hourly rainfall series according to the nearest hourly reference rain gauge. Potential evapotranspiration, estimated using the Penman-Monteith equation from daily meteorological measurements at Luxembourg airport, have been calculated for each rainfall Thiessen polygon according to the proportions of different land-use type over the polygon (Drogue *et al*., 2002). Data are available for 52 months of hourly rainfall, discharge and potential evapotranspiration from December 1996 to March 2001. The average streamflow at Steinsel during the monitoring period is 5.6 $m^3 s^{-1}$, with flows ranging from 0.07 to 40.5 $m^3 s^{-1}$.

MODEL DESCRIPTION

The WetSpa model is a grid-based distributed hydrological model for water and energy transfer between soil, plants and atmosphere (Wang *et al*., 1997; Liu *et al*., 2003). For each grid cell, the vertical is divided into four layers: vegetation zone, root zone, transmission zone and saturated zone. In the model, the hydrological processes are precipitation, interception, surface depression, surface runoff, infiltration, evapotranspiration, percolation, interflow, ground water flow and water balance in the root zone and in the saturated zone. The total water balance for a raster cell is the water balance for the vegetated, bare-soil, open water and impervious parts of each cell. This allows account to be taken of the non-uniformity of the land-use per cell, which is dependent on the resolution of the grid. The model predicts peak discharges and hydrographs, which can be defined for any numbers and locations in the channel network and can simulate the spatial distribution of catchment hydrological characteristics.

For each grid cell, the root zone water balance is modelled continuously by equating inputs and outputs. The change in soil moisture content for each time interval is determined by subtracting the volume of initial abstraction (interception and depression), surface runoff, evapotranspiration, interflow and percolation out of the root zone. The surface runoff or rainfall excess is calculated using a moisture-related modified rational method with a potential runoff coefficient which depends on land cover, soil type, slope, the magnitude of rainfall and the antecedent soil moisture (Liu, 2004). Values of potential runoff coefficient are taken from the literature and a lookup table is generated, linking values to slope, soil type and land-use classes (Liu, 2004). Evapotranspiration from soil and vegetation is calculated as a function of potential evapotranspiration, vegetation

type, stage of growth and soil moisture content. For the surface layer, actual evapotranspiration is the area-weighted mean of the land-use percentage, assuming transpiration from the vegetated parts, evaporation from the bare soil and no loss from impervious areas. Part of the potential evapotranspiration remaining after abstraction from the soil and land surfaces is lost from the groundwater as a function of groundwater storage. Finally, the total evapotranspiration is the sum of evaporation from interception and depression storage and evapotranspiration from soil and groundwater storage. The percolation out of the root zone is equal to the hydraulic conductivity which is a function of the moisture content and the soil pore size distribution index (Eagelson, 1978). Interflow occurs in the root zone after percolation and becomes significant only when soil moisture exceeds field capacity. Darcy's law and a kinematic wave approximation are used to estimate the amount of interflow generated from each cell, as functions of hydraulic conductivity, moisture content, slope angle and rooting depth.

Overland and channel flow are routed by the diffusive wave approximation (Liu *et al*., 2003). An approximate solution using a two-parameter response function, based on the average flow time and the standard deviation of the flow time, is used to route water from each grid cell to the catchment outlet or to a selected convergent point in the catchment. The flow time and its variance are determined by the local slope, surface roughness and the hydraulic radius for each grid cell. The flow path response function at the outlet of the catchment or any other downstream convergence point is calculated by convoluting the unit responses of all cells in the drainage area to form a probability density function representing the distribution of travel times. This routing response serves as an instantaneous unit hydrograph and the total discharge is obtained by a convolution integral of the flow responses from all spatially distributed precipitation excesses.

Because movement of groundwater is much slower than that of water in the surface and near surface water systems, and little is known about the bedrock, groundwater flow is simplified as a lumped linear reservoir on a small GIS derived sub-catchment scale. Considering the river damping effect for all flow components, overland flow and interflow are routed firstly from each grid cell to the main channel and are combined with groundwater flow at the sub-catchment outlet. Then the total hydrograph is routed to the basin outlet by the channel response function. The total discharge is the sum of overland flow, interflow and groundwater flow, and is obtained by a convolution integral of the flow responses from all grid cells. This approach allows the spatially distributed runoff and hydrological parameters of the basin to be used as inputs to the model; these include digital elevation data, soil type, land-use data and climatological measurements. Stream discharge data are optional for model calibration. All hydrological processes are simulated within a GIS framework.

MODEL CALIBRATION AND VALIDATION

The model was verified for the present situation before being applied to simulate the effects of river rehabilitation to mitigate flooding of the study area. Initially, model parameters were identified using GIS tools and lookup tables, which relate default model parameters to the base maps, or to a combination thereof. Starting from a 50 m × 50 m pixel resolution digital elevation map of the Steinsel sub-basin, hydrological features including surface slope, flow direction, flow accumulation, flow length, stream network and drainage area were delineated. Maps of porosity, field capacity, wilting point, residual moisture content, saturated hydraulic conductivity and pore size distribution index were determined from the soil type map. Maps of root depth, Manning's roughness coefficient, and interception storage capacity were derived from the land-use map. Specifically, the Manning roughness grid was constructed, firstly, for the hillslope area depending on the land-use category of each grid cell and then merged by the channel roughness grid containing a unique roughness value. Maps of potential runoff coefficient and depression storage capacity were obtained from the slope, soil type and land-use combinations. Due to the model grid size, cells in urban areas may not be 100% impervious; in practice, the percentage of impervious area in a grid cell was based on land-use classes, with 30% for residential areas, 70% for commercial and industrial areas, and 100% for streams, lakes and bare exposed rock. Default potential runoff coefficients for these areas were calculated by adding the impervious percentage with a grass runoff coefficient multiplied by the remaining percentage. The average downstream flow time from any cell to the outlet along the flow path is calculated by integrating the inverse of the celerity along each flow path. Similarly, the standard deviation of the flow time from each grid cell to the outlet was obtained. Then, the WetSpa model was run using the hourly time series of rainfall and potential evapotranspiration.

The model was calibrated against hourly streamflow measurements at the four stations from December 1996 to December 1999, while the period of January 2000 to March 2001 was used for model validation. The model improvement and calibration proceeded in three phases, focusing on different flow conditions. Initially, the volume of precipitation, evapotranspiration and outflow was

examined at each flow station, for which the correction factor of potential evapotranspiration was determined. Next, the interflow and groundwater flow recession coefficients were adjusted by comparing the low flow with the recession part of the flood hydrographs. The third phase of model calibration focused on improving the timing, magnitude and hydrograph shape of various flood pulses. In conjunction with this, major parameters, including channel roughness coefficient and hydraulic radius, were adjusted to achieve a best agreement with the measurements. A value of 0.04 $m^3 s^{-1}$ was obtained as the Manning roughness coefficient for the present situation by model calibration, which is typical of a clear stream without vegetation or any other major obstructions. The calibrated minimum hydraulic radius for overland flow was 0.005 m and the maximum 1.2 m for channel flow at the sub-basin outlet for a normal flood corresponding to a two-year return period. These values can be increased for extreme floods.

Based on the graphical and numerical evaluation of the modelling results, model parameters were adjusted and the model was re-run until a good match between the observed and simulated hydrographs was obtained. Figure 3 shows the observed and simulated streamflows for a compound flood at Steinsel; this was the maximum flood during the simulation period and occurred in October and November 1998. In the figure, the general evolution of the observed hydrograph is reproduced rather well. The total rainfall was 193.2 mm with measured runoff of 87.6 mm and a simulated runoff of 84.3 mm. A small flood on October 24 was followed by three large floods with observed peak discharges of 33.3, 38.8 and 40.5 $m^3 s^{-1}$. The predicted peak discharges were 34.3, 42.7 and 38.4 $m^3 s^{-1}$ with relative errors of 3.0%, 10.0% and –5.2% respectively. Figure 4 gives the observed versus simulated peak flows selected from 60 independent storm events throughout the simulation period. The high peak discharges were reproduced reasonably well, while the

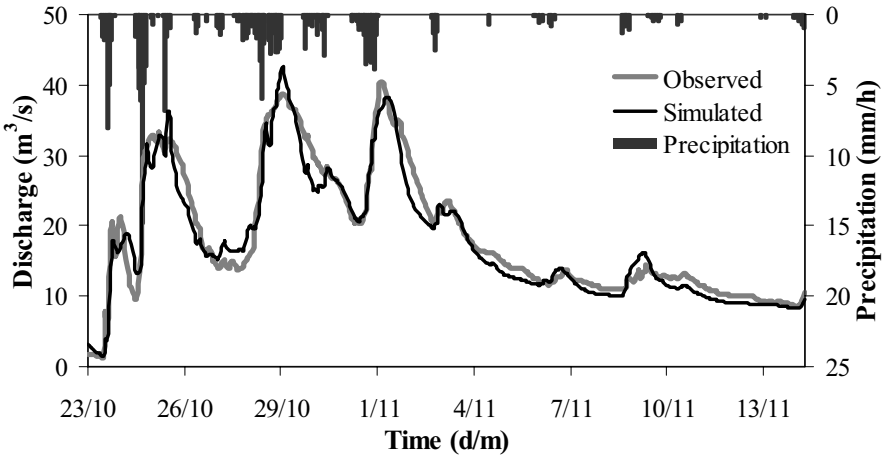

Fig. 3. *Observed and simulated hourly flows for the flood in Oct. and Nov. 1998*

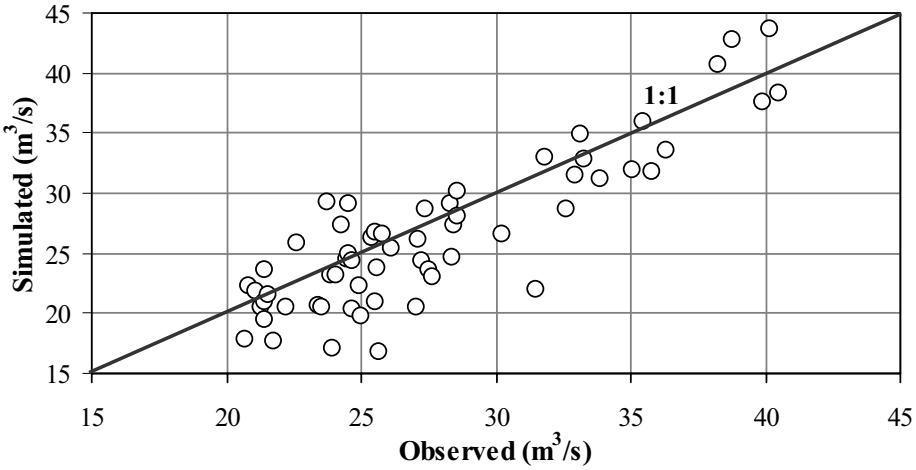

Fig. 4. *Observed versus simulated peak flows for the simulation period*

Table 1. Model performance for the calibration and validation period

Station	*Area* (km²)	*Calibration (12/1996 – 12/1999)* CR1	CR2	CR3	CR4	*Validation (1/2000 – 3/2001)* CR1	CR2	CR3	CR4
Livange	233	-0.02	0.78	0.83	0.82	-0.04	0.75	0.78	0.80
Hesperange	291	-0.03	0.83	0.78	0.87	-0.02	0.79	0.81	0.84
Pfaffenthal	350	0.02	0.81	0.82	0.92	-0.03	0.80	0.76	0.87
Steinsel	407	0.01	0.85	0.83	0.85	-0.03	0.84	0.82	0.86

estimations were slightly worse for small floods. Some points which were far from the 1:1 line might be caused by small scale thunderstorms for which the spatial distribution of rainfall was not well captured by the rainfall stations (Drogue *et al*., 2002).

Four evaluation criteria used by Drogue *et al*. (2002) were applied to assess the model performance for both calibration and validation periods at the four flow stations (Table 1). CR1 is the model bias, for which the value 0 represents a perfect simulation of the flow volume. CR2 is the Nash-Sutcliffe coefficient (Nash and Sutcliffe, 1970) for evaluating the ability to reproduce the time evolution of flows with a best value of 1. CR3 is a logarithmically transformed Nash-Sutcliffe criterion which reduces the emphasis on high flows and is, therefore, valuable for evaluating the quality of the low-flow simulations. CR4, an adapted version of the Nash-Sutcliffe criterion giving more weight to high discharges, was used to evaluate model efficiency for high flows. The numerical values of the four criteria show that the WetSpa model provides good fits to the observed hydrographs at the four flow stations with values of CR1 varying between –0.04 and 0.02, CR2 from 0.75 to 0.85, CR3 from 0.76 to 0.83, and CR4 from 0.80 to 0.92 for both calibration and validation periods.

Assessment and discussion

STREAM CLASSIFICATION

The classification of stream channels can be helpful in the interpretation and assessment of the response of stream channels to the resistance or obstruction of flow. This assessment and interpretation is helpful in deciding on which section of the basin to focus to restore streams. Usually streams are classified according to their number of tributaries and confluences. Smaller tributaries are assigned the lowest order and main rivers the highest. One of the most popular methods for assigning stream orders was proposed by Strahler (1957). The uppermost channels in a catchment with no upstream tributaries are first order. The confluence of two first-order streams gives a second-order stream and so

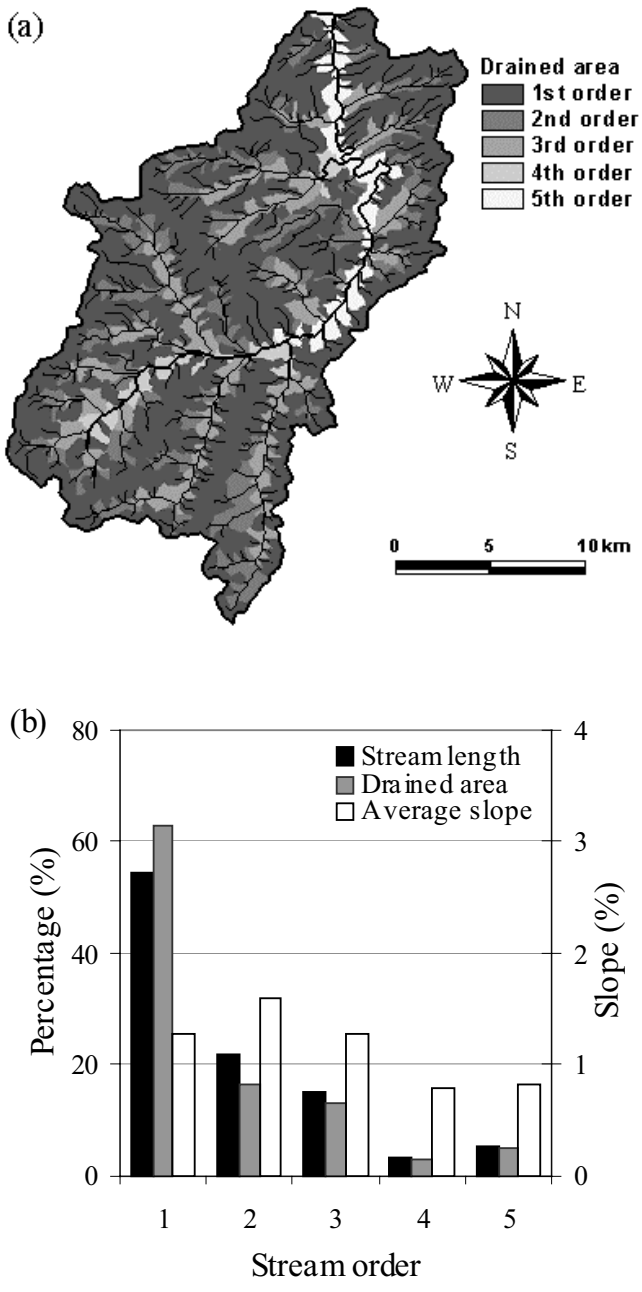

Fig. 5. *(a) Stream orders and their drained area, and (b) percentage of stream length, percentage of drained area and average slope for different order streams*

on, but the confluence of a channel with another channel of lower order does not raise the order of the stream thereafter. The main purpose in classifying the streams of the Steinsel sub-basin is to make a sound judgement about the areas of the basin that can be rehabilitated to mitigate floods. Figure 5 shows the different stream orders and their specific characteristics according to Strahler's method, extracted from a 50 × 50 m resolution DEM of the basin.

The streams of the study area were ordered from first to fifth order corresponding to the threshold value of 100 cells when delineating the stream network based on the flow accumulation theme. This implies that the flow concentration is sufficient to initiate a channel if the drainage area is greater than 0.25 km^2. Figure 5a represents the area of the sub-basin drained by different order streams. Among them, the first and second order streams drain about 322 km^2 area representing 79% of the total study area (Fig. 5b), while the length of the first and second order streams is 425 km, about 76% of the total length of the GIS-extracted stream network of the Steinsel sub-basin (Fig. 5b). Headwater streams are predominantly accumulators, processors and transporters of materials from the terrestrial system. Therefore, rehabilitating these stream channels can have significant implications in the reduction of floods in the river basin downstream. These stream channels have moderate gradients with calculated average slopes of 0.013 and 0.016 for the first and second order streams respectively (Fig. 5b). In addition, the characteristics of these headwater streams are much more influenced by riparian vegetation and geomorphology than the higher order channels downstream.

ASSESSING APPROACH

To achieve diverse habitats, environmentally acceptable river naturalisation prefers features such as non-uniform cross-sectional profiles, vegetation, meanders, islands, riffles and pools (Hansen, 1996). In addition, allowing natural rehabilitation by wood and debris falling in streams to regulate river flows is becoming an important component of current stream and river restoration (Larson *et al*., 2001). However, predicting the amount and distribution of flow obstacles in the streams is difficult; this is not uniform throughout the stream network and depends on the morphology of the river system and the dynamics of the flow. Generally, small channels have abundant wood and debris distributed randomly, affected by the density and species composition of the riparian area. Due to variable roughness and extra turbulence, estimation of flow behaviour after naturalisation is rather difficult.

Because there have been few detailed studies made in the Alzette headwaters of the channel morphology and the distribution and movement of wood and vegetation in the streams during and after floods, conceptual river rehabilitation measures proposed in this study were based on the characteristics of the basin. In the study area, the small streams originate on the plateaux with channel riparian areas characterised mainly by forest land-use, while much of the downstream area is characterised by urban settlement. The slopes of the first and second order streams are steeper than those of higher order streams (Fig. 5b), which have a potential of eroding and entraining the riparian vegetation. The mean bank-full width of these streams is generally less than 2 m, and the mean bank-full depth less than 0.5 m; these conditions are favourable for the collection of woody debris that can form obstacles and increase the resistance to the flow. Moreover, first and second order streams flowing through forest enable brushwood to be entrained in the stream. Hence, natural rehabilitation of the first and second order streams is proposed to mitigate floods in the main channels of the sub-basin downstream. Riparian and stream strategies may include increasing desirable vegetation, decreasing invasive species and increasing stream sinuosity. Four factors considered before and after river rehabilitation include change of flow resistance, stream re-meandering, change of stream slopes and of hydraulic radius.

Change in stream flows is linked directly to the change in flow resistance of the streams. Such resistance to flow reflects the rate of energy dissipation and incorporates resistance offered by in-stream vegetation and natural obstructions such as accumulation of wood and debris. The effect of vegetation and natural obstructions in the stream channels is quantified in the Manning roughness coefficient, which can increase by up to three times the previous values. (Yen, 1991; Shields and Gippel, 1995). Therefore, it is proposed to increase the Manning roughness coefficient from 0.04 to 0.1 m^3 s^{-1} in the first and second order streams, while the Manning coefficient of the higher order streams remains unchanged.

Stream re-meandering, one of the major measures for river rehabilitation and restoration, can remedy some of the consequences of former channelisation and improve the interplay between watercourses and their river valley. Typical examples are given by Hansen (1996) for river rehabilitation projects in Denmark involved re-meandering and increased inundation of the floodplains; specifically, an upper reach was altered from a 2.7 km straight and channelised channel into a new 3.2 km meandering course. Considering the non-uniformity of the stream meandering for the Alzette headwater streams, effecting an increase of 10% in channel sinuosity would increase the total length of the first and second order streams by 42.5 km.

Moreover, after rehabilitation by stream re-meandering,

the longitudinal stream slope is reduced; a 10% increase in channel sinuosity would cause a similar decrease, i.e. 0.0012, in the average channel slope of the first and second order streams. Changes in slope may also be associated with changes in channel material and in-stream vegetation, which slow down the flow and induce sediment deposition along the river channel. However, only the slope change caused by stream re-meandering is considered in this study.

Hydraulic radius is a measure of the relative channel shape; it is governed by the channel cross-section and a particular flow level. For broad and shallow channels, it is often approximated by flow depth. Although it would be logical to model the dynamic interaction between water level and channel flows from the characteristic profiles, this necessitates detailed information on the hydraulic properties of the entire channel network and such information does not exist for the Steinsel sub-basin. Hence, a diffusive wave approximation routing procedure was adopted, which assumes time-independent flow velocities parameterised as a function of the topographic gradient, which is commonly used in GIS-based flow routing schemes (Lee and Yen, 1997; Olivera and Maidment, 1999). The model determines the hydraulic radius by a power law relationship (Molnar and Ramirez, 1998), which, for discharge of a given exceedence probability, relates hydraulic radius to the drained area and is representative of the average behaviour of the cell and the channel geometry. After rehabilitation, because of the increased flow resistance, more water will be retained in the headwater streams during the rising stage of a flood event. However, this extra flood volume may be compensated partly by the extended river reaches after stream re-meandering. Accordingly, the estimation scheme for hydraulic radius remains unchanged in this study.

Once the model is verified for the present conditions, it can be applied to simulate the effect of river rehabilitation in first and second order streams in the study area. In the absence of detailed information of the hydraulic properties of the entire channel network, the changes in flow resistance, flow length and stream slope are assumed to be uniformly distributed over the headwater streams. Applying these changes gives a new roughness coefficient grid and a new channel slope grid for the first and second order streams. The new grids were then merged with the previous roughness coefficient and slope map of the sub-basin. New grids of average flow time and its standard deviation were obtained using the weighted GIS FLOWLENGTH routine, giving an extra weight of 1.1 to the first and second order streams to account for the increase of flow length for each channel cell, while the grid of flow direction and accumulation was kept unchanged. Thus, the flow response function after river rehabilitation was obtained for each grid cell.

MODEL SIMULATION

The immediate effect of river rehabilitation in the first and second order streams is to decrease the flow velocity in these channels but, once the flow enters the main channel, there is no change in velocity. However, the lower velocities in the first and second order streams have prolonged the travel time from the headwater areas to the sub-basin outlet. Figure 6a gives the average flow travel time to the sub-basin outlet in hours for the present condition, in which the flow time is less than 10 hours for the main river and up to 35 hours for

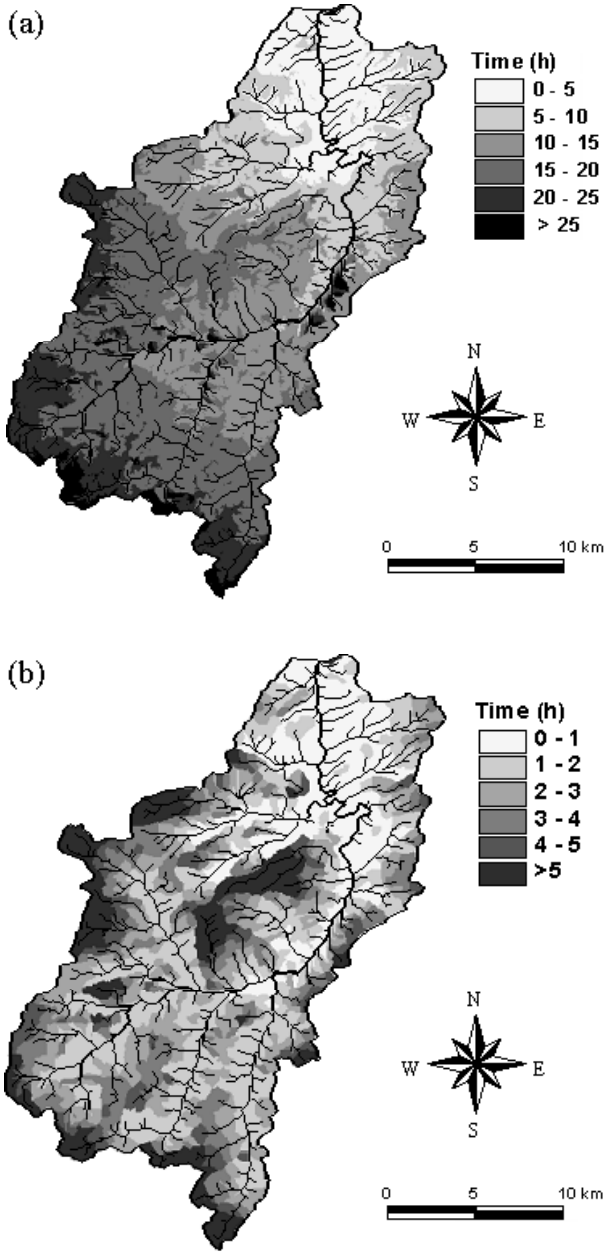

Fig. 6. *(a) Average flow travel time to the sub-basin outlet for the present condition, and (b) Increases in flow travel time after river rehabilitation*

the most remote areas. Figure 6b shows the increase in average flow travel time after river rehabilitation, in which the travel time of areas of the sub-basin that are drained by first and second order streams is delayed by several hours, while the flow time of areas drained by high order streams remains unchanged.

The changes in stream features after river rehabilitation result not only in a time delay from the headwater streams to the downstream main river but also in a reduction in peak flows at the outlet of the sub-basin. Figure 7 shows the impact of river rehabilitation on peak discharges for the compound flood event in October and November 1998, described in the model calibration. Under the proposed conceptual mitigation plan, peak discharges are reduced to 29.8, 38.2 and 35.1 $m^3 s^{-1}$, indicating a 13%, 10% and 9% reduction respectively in calculated peak discharge. These reductions occurs in the rising stage of the flood hydrograph and continue until the peak value is reached. In the recession limb, the runoff is larger than at present. This shows that the flow is stored in the headwater streams and released later during the recession stage of the flood. Figure 7 also indicates that the travel times of the peak discharges are shifted by one to two hours by the delaying effect on the water flow.

An overview of the before and after effect of river rehabilitation on peak discharges is shown in Fig. 8, for the 60 independent storm events during the entire simulation period. For all storms, peak flows are reduced by an average of 14%. This reduction is substantial and can contribute significantly to flood mitigation in the main rivers downstream.

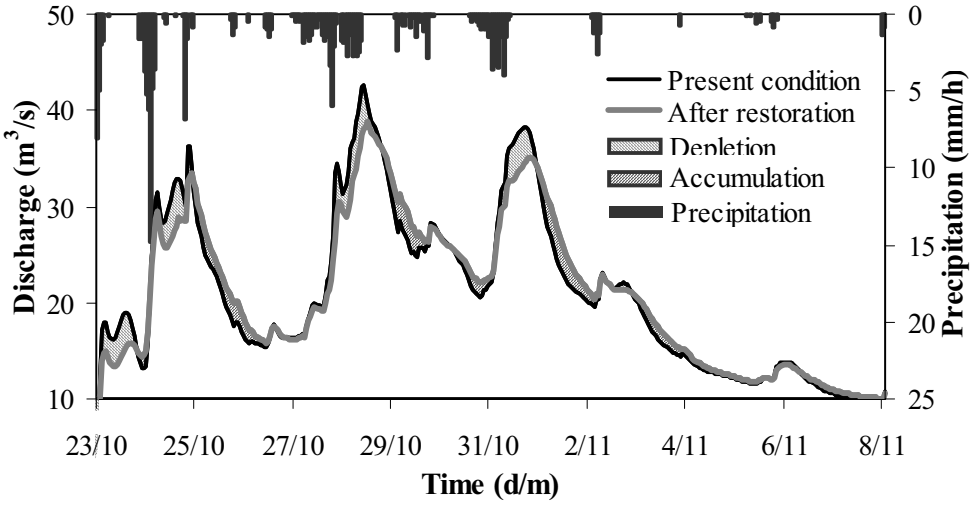

Fig. 7. *Flood events showing the effect of natural river rehabilitation*

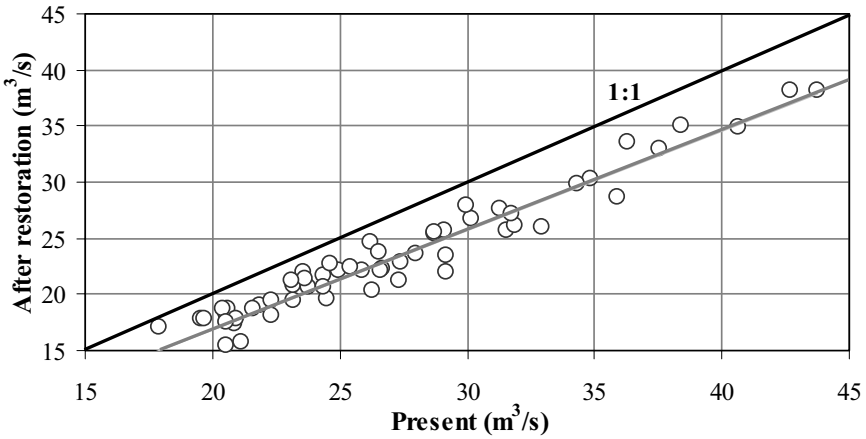

Fig. 8. *Present versus restored simulated peak discharges for the simulation period indicating a 14% reduction in average after river rehabilitation*

EVALUATION OF A FUTURE FLOOD SCENARIO

There has been a marked increase in the contribution of the westerly component of atmospheric circulation to rainfall in the Alzette basin since the 1970s (Pfister *et al*., 2000). These changes in atmospheric circulation are usually associated with increases in rainfall intensity and duration, which result in a significant increase in the winter maximum daily storm and river flow. Therefore, the model approach can be used to investigate the consequences of future climate changes and the potential effect of river rehabilitation for a given storm scenario under present land-use conditions.

Future regional climate scenarios are constructed using the outputs from HadCM3, which is the third generation coupled atmosphere-ocean general circulation model developed by the U.K. Meteorological Office, Hadley Centre (Gordon *et al*., 2000). The atmospheric component of HadCM3 has 19 levels with a horizontal resolution of 2.5° latitude by 3.75° longitude; this produces a global grid of 96 by 73 cells equivalent to about 417 km by 278 km at the Equator. Future time series of precipitation and temperature are synthesised, the latter to estimate the potential evaporation to be used, as input to the WetSpa model. The downscaling of precipitation and temperature for the study area is by the Statistical Downscaling Model (SDSM) (Wilby *et al*., 2002). Firstly, a daily statistical relationship is established between surface and upper-atmospheric circulation variables with locally observed precipitation and temperature data for the period from 1961 to 1990. Next, the SDSM model is calibrated using observations of precipitation and temperature for the baseline period together with the selected predictor variables, namely, the geopotential height and relative humidity at 500 hPa, the geopotential height and relative humidity at 850 hPa, the near surface specific humidity, the westerly wind component at 10 m elevation and the maximum temperature at 2 m height (Gebremeskel, 2003). Hourly precipitation and temperature series are extracted from the daily SDSM predictions by amplification of the hourly baseline series.

A simulated worst storm scenario in February, 2050, is selected from the SDSM predictions to study the potential effect of river rehabilitation on flood shape at the sub-basin outlet as shown in Fig. 9. The total rainfall of 72.5 mm in 18 hours with a maximum intensity of 11.3 mm h^{-1} corresponds to a winter storm with a frequency of 2% (Gebremeskel, 2003). A new grid of hydraulic radius is generated by the model with an exceedence probability of 50-year return period, which results in a maximum value of 2 m at the basin outlet, nearly double the value obtained for a normal flood with a 2-year return period. Thereafter, grids of flow velocity, average travel time and its standard deviation are created. By keeping other parameter grids the same as those used in model calibration and prediction, the outflow hydrograph at Steinsel is estimated by the WetSpa model using the input data from the selected scenario. The calculated peak discharge for this flood under the present condition is 70.1 $m^3 s^{-1}$. The estimated peak discharge at Steinsel, after river rehabilitation, is 59.5 $m^3 s^{-1}$, a 15% reduction and the peak time is delayed by 2 hours.

In terms of the volume of water volume for this scenario flood, about 1 million m^3, retained in the first two days, is released in the following four days. This water volume is stored in the first and second order riverbeds and their floodplains; the depth of water in these watercourses will be increased substantially so that, although the river

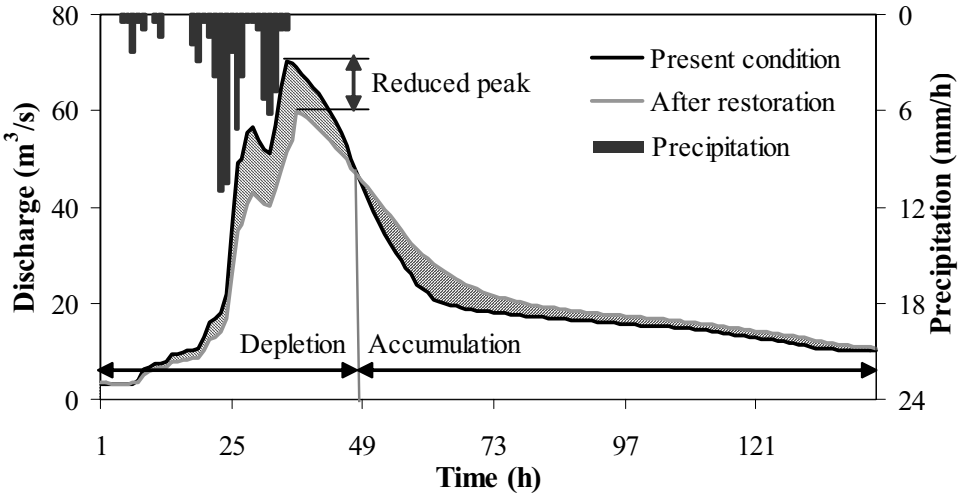

Fig. 9. *Simulated hydrograph before and after rehabilitation for a worst case scenario for SDSM in 2050*

rehabilitation may cause flooding locally this will be less dangerous and damaging than flooding of the urban areas downstream.

Discussion

In this study, an increase in roughness coefficient of 150% was assumed for the first and second order streams after river rehabilitation. Typical Manning's roughness coefficient values range from 0.08–0.12 $m^3 s^{-1}$ for minor streams with dense vegetation and irregular alignment and cross section (Chow, 1959). Much higher values have been reported in some recent river rehabilitation studies in Europe, e.g. Helmiö and Järvelä (1998) and Seara and Newson (2004). A Manning's coefficient value of 1.0 $m^3 s^{-1}$ is, therefore, feasible to reflect the stream condition after rehabilitation. However, Manning's roughness coefficients are site-specific, depending on the channel surface roughness, irregularity, shape variation, obstructions, type and density of vegetation, degree of meandering, flow depth, seasonal changes in vegetation and so on. These factors are unique to each stream reach and change in space and time. Applying a single value of roughness coefficient to all the headwater streams in this study may well misrepresent site conditions and add uncertainty to the simulations.

In this study, the flow routing is modelled by a linear approximation of the diffusive wave equation. This method assumes that flood waves propagate at a constant velocity on a river reach. The WetSpa model calculates flow velocity at each grid cell using Manning's equation as a function of roughness coefficient, slope and hydraulic radius. The hydraulic radius is estimated as a power function of the upstream drainage area of the cell and varies with flood frequencies. Parameters controlling the distribution of hydraulic radius for different flood magnitudes are adjusted at each gauging station using historical records during model calibration. Consequently, the average travel time to the basin outlet and its standard deviation can be obtained; these are location dependent and vary with flood frequencies. Since no detailed channel geometric data are available, the effects of overbank flow and flood plain storage are accounted for in the model by cautiously setting the hydraulic radius parameters for extreme flood. The resulting values are compared with measurements at different stations and adjusted through model calibration. However, such simplification may not represent the real situations under heavy flooding and may reduce the value of model validation.

In addition to the conventional rehabilitation measure of increasing natural flood storage capacities in lowland areas downstream, flood mitigation strategies in upstream areas are important (WWF, 2002) if they reduce rapid runoff on upland and riparian areas and retain more floodwater in the upstream tributaries; consequently the flood risk downstream will be mitigated. Compared with other flood control measures, river rehabilitation, by increasing channel resistance in the headwaters, provides a wide range of benefits by reducing soil erosion, increasing water quality, maintaining biodiversity and areas for recreation and so on. These strategies are, therefore, essential for integrated river basin management**.** Rehabilitation measures are, however, feasible and can be carried out gradually over a long period, alongside other changes such as stopping deforestation, using buffer zoning and strips, planting trees alongside the river channel, providing tree barriers and other engineering measures.

This study focuses on the possible river rehabilitation effects on the Steinsel sub-basin. It comprises 34.7% of the Alzette basin (1175 km^2) and is only 0.22% of the Rhine River basin (185000 km^2). Simulations in this study show that natural river rehabilitation in the headwaters can prolong the time of flow and cause a remarkable reduction in the flood peaks in the main channels downstream. These measures, applied throughout the vast headwater areas of the Rhine basin, may mitigate the flood risk on the main river channels significantly. This is particularly important for the delta downstream; this depends strongly on flood defence strategies for the entire river basin and the time of peaks in all the tributaries. However, the impact of river rehabilitation of headwater areas cannot be assessed simply by amplifying the results obtained from a small sub-catchment. Collection of detailed data and studies on the complex flow systems are required in this respect.

Concluding remarks

This paper presents the effects of river rehabilitation on flood reduction in the Steinsel sub-basin of the Alzette River basin, Grand-Duchy of Luxembourg. A conceptual method to account for the effect of in-stream vegetation and channel re-meandering is focused on the first and second order streams ordered according to Strahler's method and implemented using the WetSpa model, applied in a GIS environment. Model calibrations and validation have shown the model to give satisfactory results.

After river rehabilitation, the simulation results indicate a decrease in peak discharge of up to 14% and a delay in the occurrence of flood peaks of as much as 2 hours. The discharge is reduced during the rising limb of the flood hydrograph but it increases during the falling limb of the hydrograph; this results in longer sustained flows than under present conditions. Although river rehabilitation reduces

large floods in the main stream channels, local flooding may occur in the headwater stream areas. It is concluded that river rehabilitation, designed to increase flow resistance in the headwaters, restores more natural conditions, enables watercourses locally to flow over their flood plains and has a positive influence in reducing the risk of flooding downstream, where the consequences may be more severe due to the size of the river basin and the magnitude of the discharge. This work focused on the beneficient effects of river rehabilitation for flood reduction in the Steinsel sub-basin. However, this study did not cover beneficial and adverse effects on the ecology and morphology of river basins.

References

Chow, V.T., 1959. *Open-Channel Hydraulics*, McGraw-Hill, New York, USA. 680pp.

Drogue, G., Leviandier, T., Pfister, L., El Idrissi, A., Iffly, J.F., Hoffmann, L., Guex, F., Hingray, B. and Humbert, J., 2002. The applicability of a parsimonious model for local and regional prediction of runoff. *Hydrolog. Sci. J.*, **47**, 905–920.

Eagelson, P.S., 1978. Climate, Soil, and Vegetation, a simplified model of soil moisture movement in liquid phase. *Water Resour. Res.*, **14**, 722–730.

Gebremeskel, S., 2003. *Modelling the effect of climate and land-use changes on hydrological processes: An integrated GIS and distributed modelling approach*. Doctoral Thesis, Free University of Brussels, Belgium.

Gordon, C., Cooper, C., Senior, C.A., Banks, H., Gregory, J.M., Johns, T.C., Mitchell, J.F.B. and Wood, R.A., 2000. The simulation of SST, sea ice extents and ocean heat transports in a version of the Hadley Centre coupled model without flux adjustments. *Clim. Dynam*., **16**, 147–168.

Hansen, H.O. (Ed.), 1996. *River Restoration, Danish experience and examples*. Ministry of Environment and Energy, National Environmental Research Institute, Silkeborg, Denmark.

Helmiö, T. and Järvelä, J. 1998. Assessing the hydraulic performance in river rehabilitation projects - Myllypuro Brook case study. In: *Proc.XX Nordic Hydrological Conference,* J. Kajander(Ed.), Helsinki, Finland. 357–364.

Larson, M.G., Booth, D.B. and Morley, S.A., 2001. Effectiveness of large woody debris in stream rehabilitation projects in urban basins. *Ecol. Eng*., **18**, 211–226.

Lee, K.T. and Yen, B.C., 1997. A geomorphology and kinematic-wavebased hydrograph derivation. *J. Hydraulic Eng.- ASCE*, **123**, 73–80.

Liu, Y.B., 2004. *Development and application of a GIS-based hydrological model for flood prediction and watershed management*, Doctoral Thesis, Free University of Brussels, Belgium.

Liu, Y.B., Gebremeskel, S, De Smedt, F, Hoffmann, L. and Pfister, L., 2003. A diffusive transport approach for flow routing in GIS-based flood modelling. *J. Hydrol.*, **283**, 91–106.

Molnar, P. and Ramirez, J., 1998. Energy dissipation theories and optimal channel characteristics of river networks. *Water Resour. Res*., **34**, 1809–1818.

Morris, S.E., 1995. Geomorphic aspects of stream-restoration. *Phys. Geogr.,* 16, 444–459.

Nash, J.E. and Sutcliffe, J.V., 1970. River flow forecasting through conceptual models. Part I, a discussion of principles. *J. Hydrol.*, **10**, 282–290.

Olivera, F. and Maidment, D.R., 1999. Geographic information system (GIS)-based spatially distributed model for runoff routing. *Water Resour. Res*., **35**, 1155–1164.

Pfister, L., Humbert J. and Hoffmann L., 2000. Recent trends in rainfall-runoff characteristics in the Alzette river basin, Luxembourg. *Climatic Change,* **45**, 323–337.

Pfister, L., Humbert, J, Iffly, J.F. and Hoffmann, L., 2002. Use of regionalised stormflow coefficients in view of hydro-climatological hazard mapping. *Hydrolog. Sci. J*., **47**, 479–491.

Seara, D.A. and Newson, M.D., 2004. The hydraulic impact and performance of a lowland rehabilitation scheme based on pool-riffle installation: The river Waveney, Scole, Suffolk, UK. *River Res. Appl.*, **20**, 847–863.

Shields, F.D. and Gippel, C.J., 1995. Prediction of effects of woody debris removal on flow resistance. *J. Hydraul. Div. ASCE*, **121**, 341–354.

Strahler, A.N., 1957. Quantitative analysis of watershed geomorphology. *Trans. Amer. Geophys. Un.*, **38**, 913–920.

Wang Z., Batelaan, O. and De Smedt, F., 1997. A distributed model for Water and Energy Transfer between Soil, Plants and Atmosphere (WetSpa). *Phys. Chem. Earth*, **21**, 189–193.

Wilby, R.L. and Dettinger, M.D., 2000. Steamflow changes in the Sierra Nevada, California, simulated using a statistically downscaled General Circulation Model Scenario of climate change. In*: Linking climate change to land surface change,* S.McLaren and D.Kniveton (Eds.), Kluwer, The Netherlands. 6.1–6.20.

WWF, 2002. *Managing floods in Europe: The answers already exist*. WWF Background Briefing. Paper 26, Brussels, Belgium.

Yen, B.C., 1991. Hydraulic resistance in open channel. In, *Channel flow resistance, Centennial of Manning's formula,* B.C. Yen (Ed.), Water Resources Publishers, Littleton, Colorado USA. 1–135.